JOURNAL OF CATALYSIS 132, 524–535 (1991)

In Situ Cell for Combined XRD and On-line Catalysis Tests: Studies of Cu-based Water Gas Shift and Methanol Catalysts

B. S. CLAUSEN, G. STEFFENSEN, B. FABIUS, J. VILLADSEN, R. FEIDENHANS'L,* AND H. TOPSØE

*Haldor Topsøe Research Laboratories, DK-2800 Lyngby, Denmark; and *Risø National Laboratories, DK-4000 Roskilde, Denmark*

Received April 21, 1991; revised August 7, 1991

A newly developed *in situ* X-ray diffraction (XRD) cell has been used to obtain information on the structure of binary Cu–Zn and ternary Cu–Zn–Al catalysts during reduction and water gas shift and methanol synthesis. A major advantage of the cell is that it also serves as an ideal plug flow catalytic reactor such that realistic catalytic and structural information can be obtained *simultaneously* on the *same* sample. The cell can be operated both at high temperatures and high pressures. Direct methanol activity tests confirmed the suitability of the cell. By use of X rays from a synchrotron source, dynamic studies on the time scale of seconds have been demonstrated. This feature was used to study the phase transformation occurring during the activation of the calcined catalysts. In the active catalysts, Cu metal is the only crystalline Cu phase observed, and the formation of this phase is seen to be closely related to the disappearance of CuO in the calcined catalyst. The XRD results provide detailed information on the nucleation and growth processes. The variation in the water gas shift activity appears to correlate with the changes in the copper surface area.

1. INTRODUCTION

The importance of applying *in situ* techniques to study catalysts cannot be overemphasized, since both the surface and the bulk structures of many catalysts depend intimately on the reaction conditions (gas composition, temperature, pressure, etc.). Thus, in order to establish relationships between the catalyst properties and the catalytic activity, it is necessary to employ techniques that allow a study of these properties while the catalytic reaction takes place.

X-ray diffraction (XRD) is one of the most commonly applied techniques to provide information on the crystalline phases in heterogeneous catalysts, but the vast majority of the XRD studies reported in the past have not been carried out *in situ* but typically in air after removal of the catalysts from the reactor. In order to overcome this problem, several approaches have been proposed and their applications have provided much new insight regarding the structure of catalysts under synthesis conditions (see, e.g., Refs. (*1–14*)). In spite of this progress, it has been difficult to find solutions where both *ideal* XRD patterns and *ideal* catalytic activity measurements can be recorded *on-line* on the *same* sample. The solutions, which previously have been described for performing *in situ* XRD studies, typically have one or more limitations related to: (*i*) the necessity of transferring the sample from the reaction zone (i.e., the XRD and catalytic tests are not performed under identical conditions), (*ii*) difficulties in operating at the high temperatures and pressures commonly encountered in catalysis, (*iii*) inhomogeneities in sample and system temperature (e.g., due to the presence of cooled windows), (*iv*) the presence of large dead volumes, (*v*) the absence of gas flow through the sample or poorly defined flow and concentration profiles, (*vi*) difficulties in ensuring that the catalysis is carried out on exactly the same fraction of the sample as probed by XRD, (*vii*) difficulties in ensuring ideal conditions

0021-9517/91 $3.00

for the catalytic tests (e.g., ideal plug flow conditions), and (*viii*) the use of construction materials which may contribute to the catalysis or the XRD pattern, or which may not be chemically stable when exposed to many synthesis gases.

By use of very thin glass and quartz capillary tubes as combined XRD cells and catalytic microreactors, the above limitations have been reduced significantly. Lindemann capillary tubes have been used for decades as sample holders in normal *ex situ* X-ray powder diffraction studies (see, e.g., Ref. (*15*)), but to the best of our knowledge such tubes have not been used for *in situ* studies of catalysts with gas flowing through the tubes at elevated temperatures and pressures.

The present paper describes in detail the new *in situ* XRD cell and gives some examples of how the application of this cell may provide new insight into the genesis and structure of methanol and water gas shift catalysts. Some preliminary results and design features have been presented recently (*16, 17*). Both the industrial low-temperature water gas shift and methanol synthesis catalysts consist of a combination of Cu and Zn oxides to which alumina is added to stabilize a high active surface area of the system. Although numerous investigations have been performed on methanol catalysts, the structure of the active catalysts, the nature of the active sites, and the reaction mechanism are still subject to considerable controversy (see, e.g., Refs. (*18–21*)). For example, it has been proposed that Cu^+ species strongly interacting with the ZnO phase are present in high abundance in the catalysts during methanol synthesis (see, e.g., Ref. (*18*)). Recently, *in situ* XAFS studies (see, e.g., Refs. (*22–26*)) have shown that the predominant part of Cu in typical catalysts is present in the metallic state. Also, XRD studies of the reduced form of the catalysts have reached the same conclusions (see, e.g., Refs. (*27, 28*)). In the literature there is an ongoing discussion as to whether the methanol activity simply parallels the surface area of the Cu metal particles (*19, 20, 29, 30*) or if the oxidic support plays a more active role, for example, via Schottky junctions at the interphase between the Cu metal and the support (*31, 32*). Furthermore, the support may influence the methanol synthesis activity in other ways (*33*). For example, ZnO has been proposed to play the role of a reservoir for hydrogen and to promote hydrogen spill-over (*21, 34*).

2. CELL DESIGN

The reaction cell (Fig. 1) consists of a capillary tube made of quartz or glass (other low absorbing materials like carbon or silicon could be used) connected to stainless steel tubes via stainless steel tube fittings. This constitutes leak-tight in- and outlets of gases, as well as fixation of the capillary tube in the X-ray beam. The dimensions of the capillary depend on the specific application, but typically the wall thickness was 0.01 mm and the outer diameter 0.4 mm. The catalyst powder is loaded between two pieces of quartz or glass wool to fix the catalyst bed in the capillary. The sample is heated (or cooled) by passing a stream of hot (cold) gas (e.g., air or N_2) over the capillary tube. In order to minimize temperature nonuniformity along the catalyst bed in the capillary, a small X-ray transparent hood made of Kapton foil is surrounding the capillary and the inlet of the hot (cold) gas. The temperature is monitored by means of a thermocouple located about 1 mm from the sample. The desired temperature was obtained by regulating either the current to the electric resistance heating the gas stream or by adjusting the flow rate of the hot (cold) gas. The temperature of the heating gas could be regulated within 0.1 K by use of an electronic regulation device (Eurotherm).

The temperature profile along the tube was mapped by locating a thin (0.2 mm) thermocouple at various positions inside the tube. In the temperature range from 373 to 673 K, the temperature varied less than 3 K over a 20-mm zone along the tube. As an additional test, the melting of a Pb powder in the tube

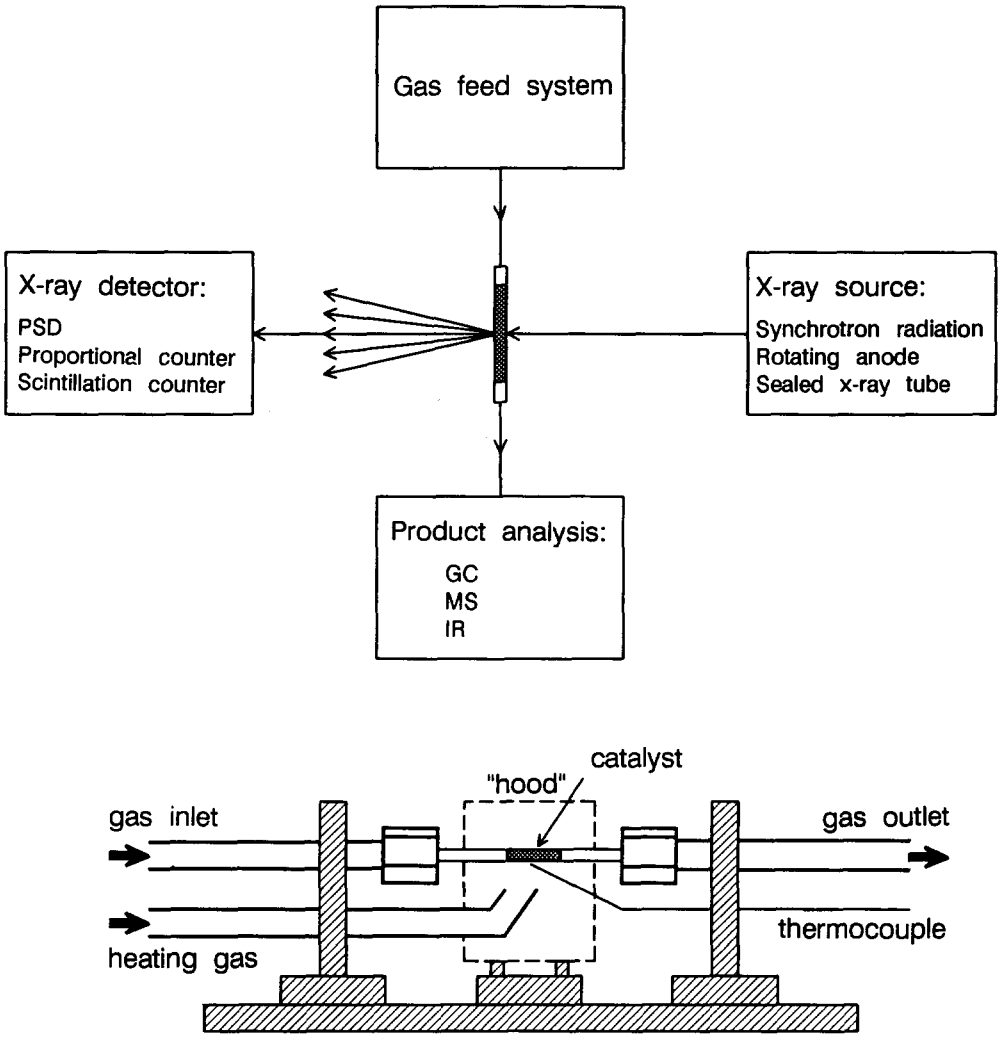

FIG. 1. Schematic drawing (not to scale) showing the combined XRD *in situ* cell and catalytic plug flow reactor. The actual dimensions are about 100 mm × 50 mm × 30 mm.

was followed by XRD. The diffraction lines were observed to disappear completely at 603 K, in good agreement with the known melting temperature (600.5 K) for Pb. The heating and cooling of the sample are exceedingly rapid (from RT to 673 K in a few seconds) due to the extremely small mass of the reaction cell and the efficient heat transfer between the gas and the capillary tube.

A versatile feed gas system equipped with electronic mass flow meters and pressure controllers was used to provide synthesis gas to the reaction cell at the desired pressure and flow rates. The products from the catalytic reaction are analyzed *on-line* at the outlet by use of a gas chromatograph, a mass spectrometer, or infrared detectors. In certain catalysis experiments it may be necessary to take into account the pressure drop over the catalyst bed. Using a sieve fraction of 105 to 150 μm, a 2-cm bed length, and a space velocity of 53,000 h^{-1}, a pressure drop

of about 5 cm Hg was typically measured at ambient pressure.

The present capillary tubes have been used at temperatures up to about 725 K and pressures up to around 5 MPa. If desired this temperature and pressure range can be expanded by choosing other materials and/or dimensions of the capillaries. From a safety point of view, it should be recalled that although the mechanical strength of various glass types is similar to that of many metals, small imperfections (inclusions, surface scratches, etc.) in the glass may substantially reduce the load at which the glass breaks. It is therefore not possible *a priori* to give exact upper limits for the conditions at which specific tubes are safe to use.

The reaction cell, as illustrated in Fig. 1, is made adjustable with respect to the length of the capillary to compensate for thermal expansion (a u-tube configuration may also be used for this purpose). The tube and hood holders are mounted on sledges running on a small optical bench. The setup can be mounted either vertically or horizontally on the goniometer, depending on the type of diffractometer. The dimensions of the reaction cell are so small that it fits into most conventional diffractometers and on goniometers at synchrotron radiation facilities.

The diffracted X rays were in some of our studies detected by means of conventional proportional or scintillation counters in an angle dispersive geometry. However, in order to study dynamic phenomena, position sensitive detectors were used (gas filled wire detectors or photo diode arrays) since they give improved counting statistics such that time resolved studies can be carried out on the time scale of seconds.

3. EXPERIMENTAL

The present measurements with the *in situ* cell were made at the DORIS II storage ring on the D4 beam line at HASYLAB, Hamburg, Germany. The X rays were monochromatized by a Ge(111) crystal scattering in the horizontal plane. The wave length of 0.14 nm was chosen to prevent fluorescence from Cu in the samples. The diffracted X rays were detected by use of an Ar-CH_4 gas filled position sensitive wire detector (MBraun GmbH) with 45% efficiency at 0.154 nm and a resolution of 50 μm. From measurements of highly crystalline SiO_2 it was found that the angular resolution is essentially given by the diameter of the capillary tube and the distance from the sample to the detector. In the present study we typically have $\Delta 2\theta = 0.045°$.

The *ex situ* XRD powder diffraction experiments were performed on a flat sample using Cu$K\alpha$ radiation generated at 40 kV and 40 mA on a Phillips vertical X-ray diffractometer which was equipped with an automatic divergence slit, diffracted beam monochromator, proportional counter, and pulse-height analyzer. A scan speed of 1° 2θ/min was used.

A series of binary methanol catalysts with Cu/(Cu + Zn) atomic ratios between 0 and 1, as well as a ternary $Cu/ZnO/Al_2O_3$ industrial type catalyst with a Cu/(Cu + Zn) ratio of 0.7, were investigated. The binary catalysts were prepared by coprecipitation from the metal nitrates as described in detail in Ref. (*35*). After the samples were dried and calcined, about 2 mg of catalyst powder (sieve fraction 106 to 150 μm) was loaded in the capillary tubes. The reduction was carried out in a flow (5 Nml/min) of 0.25% CO, 0.25% CO_2, and 4% H_2 in Ar at ambient pressure. The catalyst was heated at a rate of 10 deg./min up to 373 K and kept at this temperature for 1 hr and then heated to 493 K at a heating rate of 0.5 deg./min. After reduction, the gas was changed to a methanol synthesis gas mixture (4.6% CO, 4.7% CO_2, 3.1% Ar, balance H_2). The effluent gas from the capillary tube was analyzed *on-line* by use of a gas chromatograph (HP 5890) with a double analyzing system. The components were separated using a column system consisting of a Porapak N and a molecular sieve 13X column. H_2, Ar, CO, and CO_2 were detected with a TCD and methanol and other products with a FID. The *in situ* XRD diagrams were recorded at 2–3 min intervals

TABLE 1

Comparison of Methanol Synthesis Data Obtained in the *in Situ* Cell with those of a Laboratory Pilot Reactor

Component	Concentration (vol%)[a]		
	In situ cell		Lab. pilot reactor
	0.1 MPa	3 MPa	3 MPa
H_2	n.a.	n.a.	86.93
CO	4.6	4.5	4.85
CO_2	4.7	4.3	4.23
CH_3OH	0.01	0.3	0.34

Note. n.a., not analyzed.

[a] $Cu/ZnO/Al_2O_3$ catalyst, SV = 30,000, T = 493 K, inlet gas composition: 4.6% CO, 4.7% CO_2, 3.1% Ar, balance H_2.

during reduction and at synthesis conditions. For the dynamic studies about 5 wt% of W powder was mixed with the catalyst in order to have an internal standard.

4. RESULTS AND DISCUSSION

a. *Capabilities of the Combined* In Situ *Cell/Catalytic Reactor*

In order to relate directly structural and catalytic information it is desirable to have available an *in situ* XRD setup which *on-line* can provide *simultaneously* XRD and catalytic information on the *same* sample. This means that the XRD cell must ideally also serve as a catalytic reactor and must therefore simultaneously satisfy X-ray diffraction and catalytic reactor criteria. The present capillary tube concept shown in Fig. 1 appears to meet these criteria.

From a catalytic reactor point of view, it is an advantage that the capillary tube concept has the same geometry as ordinary tubular test reactors. Thus, the catalytic results obtained in the cell are directly comparable with those obtained in ordinary catalytic test reactors. The design eliminates the problems encountered in many previous cells arising from large dead volumes or the presence of significant temperature and concentration profiles over the sample. Table 1 summarizes the gas chromatograph data obtained when analyzing the effluent gas from the glass capillary during synthesis at 0.1 MPa and 3 MPa, respectively. The results at 3 MPa and 493 K show that the catalyst in the capillary is producing about 0.3% CH_3OH at a space velocity of 30,000 h^{-1}. As shown in Table 1 this conversion compares very well with that obtained in a laboratory pilot reactor at similar conditions. This confirms the expectations that the *in situ* XRD cell is well suited for providing simultaneous catalytic information, and thus many new studies of relationships between catalyst structure and activity are possible. Such studies are now in progress.

The possibility of going to high pressures and high temperatures is an important feature of the cell for applications in catalysis. The good temperature uniformity and the fast temperature response (*vide supra*) is also an advantage in many catalytic and kinetic studies since, for example, unwanted surface or bulk reactions during heating and cooling can be minimized. An example of time resolved studies will be discussed in Section 4.c.

The X-ray diffraction performance of the *in situ* cell should in principle be good, since the use of capillaries is well known from the classical Debye–Scherrer method. Thus, the *in situ* cell is well suited for the study of both supported and unsupported catalysts. The XRD performance was tested by comparing the diffractograms obtained using the cell with those obtained using an ordinary *ex situ* powder diffraction setup. Figure 2(a) shows the diffractogram of the ternary Cu/

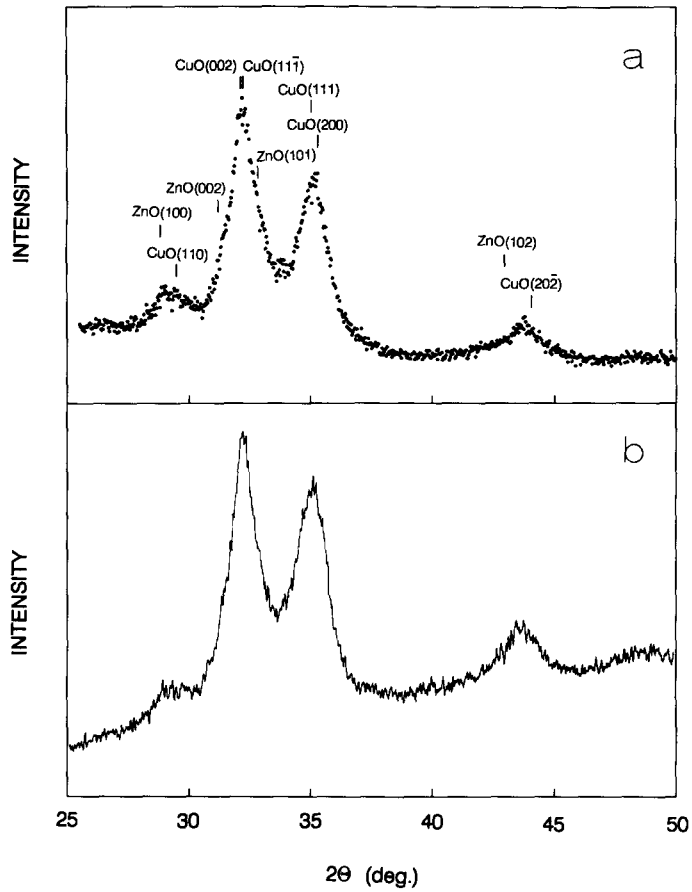

FIG. 2. (a) XRD diffractogram of a calcined $CuO/ZnO/Al_2O_3$ methanol synthesis catalyst recorded in the capillary tube at room temperature. The diagram was obtained in about 120 s using synchrotron radiation and a position sensitive detector. The bars in the diagrams indicate the position of the assigned components. (b) XRD diffractogram of the calcined, ternary catalyst recorded in reflection geometry using the Cu$K\alpha$ radiation from a sealed X-ray tube and a proportional counter. The 2θ scale is recalculated to correspond to $\lambda = 0.140$ nm.

ZnO/Al_2O_3 catalyst in the calcined state obtained with the capillary setup. For comparison, Figure 2(b) shows the diffractogram of the same catalyst using the standard commercial sample holder and diffractometer. It is clear that the present *in situ* concept can provide data of similar resolution and quality as those obtained on ordinary setups.

The absorption from the Lindemann glass is typically around 10%, whereas the absorption from the catalyst is typically 85% or more depending on its composition. As a result the X-ray beam will generally not probe the catalyst uniformly, but preferentially at the outermost parts (see, e.g., Ref. (*15*)). This may in certain cases be a problem, but it can be minimized by reducing the diameter of the tube or by diluting the catalyst with an X-ray transparent material. Nevertheless, due to the plug flow conditions and the uniformity in temperature, no significant radial concentration gradients in the solid are expected and for most practical purposes, the solid probed by XRD is that contributing to the catalysis.

In XRD studies it is in general important to minimize the effects of preferred orientation of the sample crystallites (see, e.g., Ref. (*15*)). With the *in situ* cell such effects may

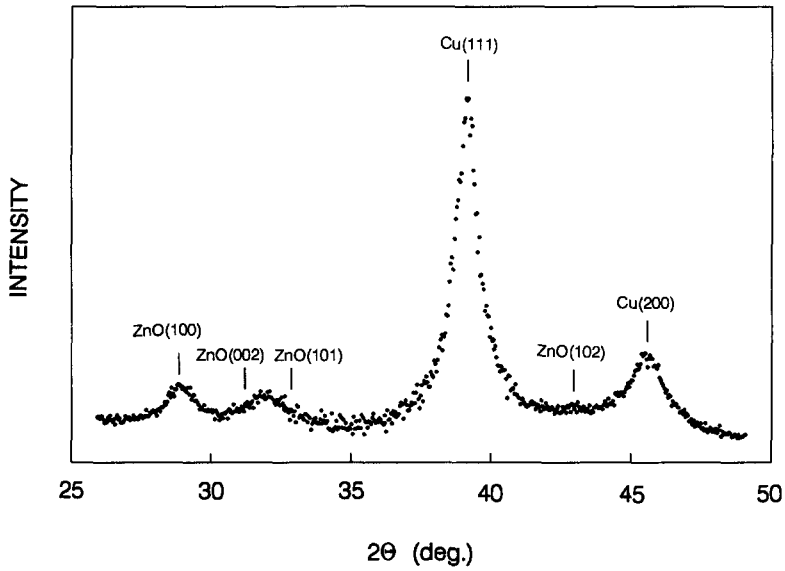

FIG. 3. *In situ* XRD diffractogram of the ternary catalyst during methanol synthesis at 493 K and 3 MPa. The diagram was obtained in about 120 s using synchrotron radiation.

become important depending on parameters like the anisotropy of the crystallites and the ratio of the particle size to tube diameter. However, for the present catalyst samples, these effects were insignificant, as seen from a comparison of Figs. 2(a) and (b). This was further confirmed in an independent study by comparison with the diffractograms from catalysts in sealed-off capillaries in a stationary geometry and with those obtained employing a rotational motion. Thus, investigations of the absolute intensities and quantitative XRD analysis are also possible. If for certain systems orientation problems arise, the round table on which the present reaction cell is mounted can be modified such that the whole setup oscillates to improve the intensity statistics.

Finally, it could be mentioned that while the present *in situ* on-line setup has been developed for XRD studies, the concept has also been used with small modifications for making *in situ* measurements with other techniques, like EXAFS.

b. Structure of Calcined and Activated Catalysts

The diffractograms of the calcined catalyst (Fig. 2) show two intense, broad lines, one at around $2\theta = 32.2°$ and one at around $2\theta = 35.1°$, as well as two weaker lines at about $2\theta = 29°$ and $2\theta = 44°$. In accordance with previous studies (see, e.g., Refs. (*27, 28*)), these results indicate that ZnO and CuO phases are present in the catalyst after calcination. Since the most intense ZnO lines overlap with lines from the CuO phase, a detailed analysis of the lattice parameter of the ZnO phase may be ambiguous, and thus it is difficult to conclude solely from these experiments if part of the copper could be substituted into the ZnO phase in the calcined catalyst or if all of the copper exists as separate CuO particles. The studies of the reduction process (Section 4c) indicate that for the present catalyst, significant amounts of Cu cannot be present in the ZnO. This is in accordance with conclusions from EXAFS experiments (*35*). No lines due to an aluminum phase in the catalyst can be resolved in the diffractogram, indicating that this element is present in a microcrystalline or X-ray "amorphous" phase.

Figure 3 shows the diffractogram of the ternary catalyst recorded at high pressure (3 MPa) and temperature (493 K) during methanol synthesis. The diffraction lines at $2\theta = 39.2°$ and $2\theta = 45.6°$ reveal that metallic

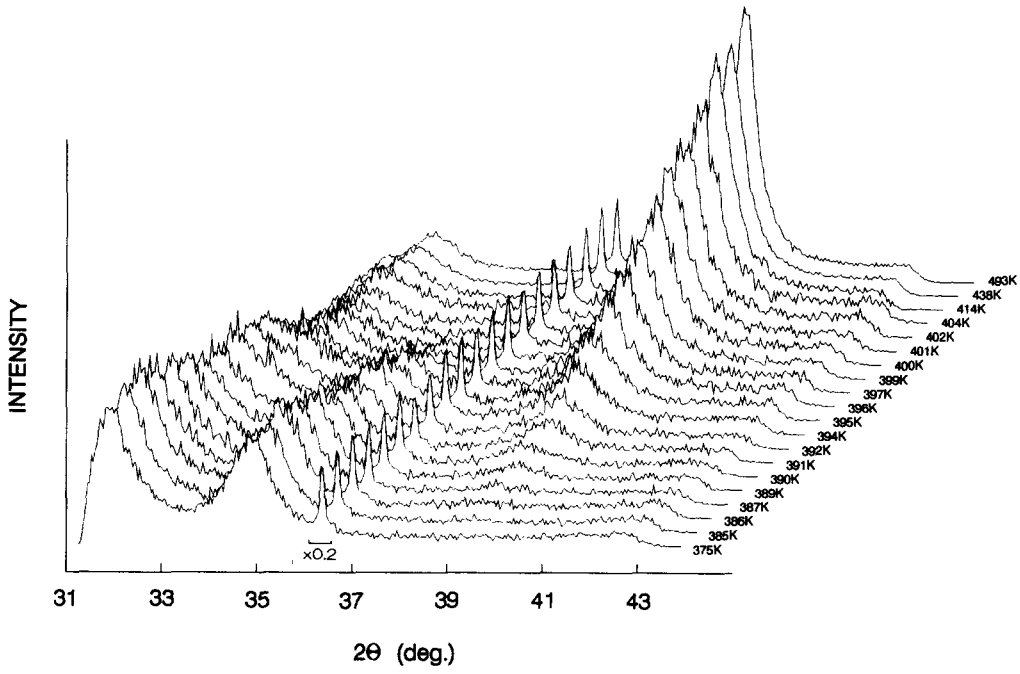

FIG. 4. 3D plot of the *in situ* XRD diagrams as a function of the reduction temperature of the binary catalyst with Cu/(Cu + Zn) = 0.80. The diffractograms were recorded on-line during the reduction and the collection time per diagram was about 60 s Tungsten (line at $2\theta = 36.45°$) was included as internal standard.

Cu crystallites are present in the ternary catalyst at methanol synthesis conditions. From a line profile analysis of the Cu(111) diffraction line, it is estimated that the average Cu metal crystallite size is about 9.5 nm. As shown in detail below, the Cu crystallite size will depend on both the type of catalyst and on the conditions of the reduction process. The presence of metallic Cu has also been reported in previous *in situ* XRD studies (see, e.g., Refs. (*11, 18, 27, 28*)) and other studies (*19–26, 29, 30*) of reduced methanol catalysts. Although we cannot exclude the presence of other Cu and Zn structures, especially if present as microcrystalline or "amorphous" species, the present XRD results do not provide support for the previous proposal (*18*) that Cu^+ dissolved in ZnO is an abundant form of copper in these catalysts. In order to shed further light on this important problem, quantitative XRD analysis of the various catalysts at synthesis conditions is presently being carried out.

c. On-line Time Resolved Studies during Reduction and Catalytic Test Conditions; Catalytic Implications

By making *on-line* time resolved studies it has been possible to follow the processes occurring during the activation of both the binary and ternary catalysts. The results for the different catalysts show similar behavior, and the studies of the binary catalyst with a Cu/(Cu + Zn) ratio of 0.80 will be discussed in detail below. The diffractograms recorded during the activation process are displayed in Fig. 4 as a function of the reduction temperature. The disappearance of the CuO lines and the gradual appearance of the Cu(111) line are clearly observed. Concurrent with the increase in the intensity the width of the Cu(111) line is found to decrease. Due to the changes in the line width quantitative information about the phase composition is most conveniently obtained by analyzing the integrated intensities. The integrated intensities of the

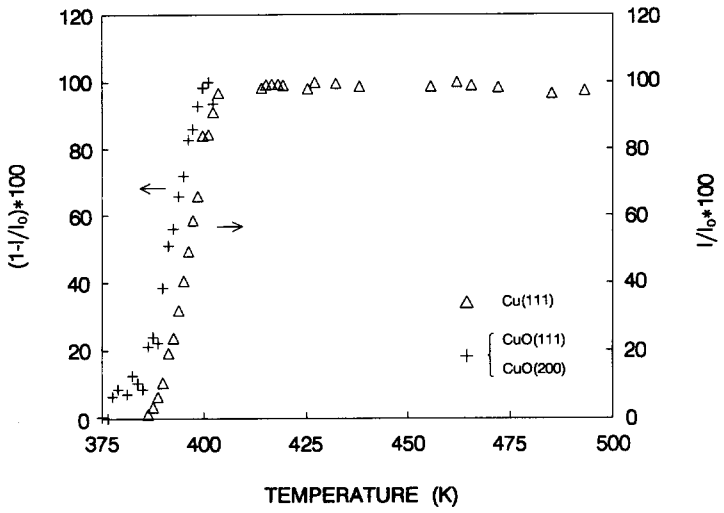

FIG. 5. Changes in the integrated intensities of CuO((111) and (200)) and Cu(111) occurring during catalyst reduction. Data from the on-line, time resolved diffractograms in Fig. 4.

Cu(111) and the overlapping CuO(111) and (200) diffraction lines (normalized to the intensity of the W(110) line) are shown in Fig. 5. The intensities have also been normalized with respect to the maximum value (I_0) measured for each phase. In order to facilitate a comparison of the intensities of the CuO and Cu phases, the integrated intensity for the CuO lines has been plotted as $1 - I/I_0$.

It is immediately clear that the two curves are almost identical. Thus, the formation of Cu is to a large extent directly related to the disappearance of CuO and as discussed below there is no evidence for significant amounts of Cu metal being produced from other precursors like, for example, Cu dissolved in ZnO.

There are some interesting differences between the CuO and Cu XRD intensity curves. First of all, crystalline CuO is noted to be reduced already at 375 K without crystalline Cu metal being observed yet. Second, the integrated Cu intensity continues to increase at temperatures slightly above that where CuO reduction has terminated. These findings can be rationalized if we consider that during the reduction process, crystalline CuO is first reduced to yield "X-ray amorphous" small metallic Cu crystallites which subsequently sinter to larger "X-ray visible" Cu particles. Thus, the observed disappearance of CuO without Cu metal being observed is explained by the Cu metal particles produced still being too small to give rise to a diffraction pattern. The observed continued increase in Cu metal intensity after completion of CuO reduction is similarly explained by some continued sintering of small Cu particles into the range where they give rise to a detectable diffraction signal. Additional support for the above explanations is obtained by analyzing the change in the Cu(111) line width, which provides information about the changes in the Cu metal particle size. The results (Fig. 6) show a dramatic increase in particle size during the initial stages of reduction. In fact, an extrapolation of the Cu metal crystallite size to the onset temperature of CuO reduction is below the typical detection limit for XRD (2.5–3.0 nm). The observation that the CuO crystallites apparently reduce to smaller Cu metal particles indicates that one has a situation where large oxide particles break up into several small metal particles. Such behavior is observed, for example, when magnetite is reduced to metallic iron in ammonia synthesis catalysts (*36, 37*).

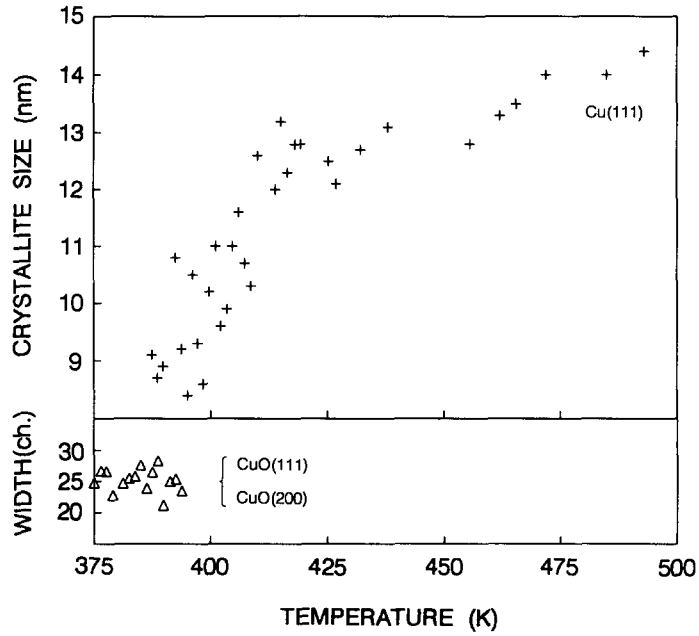

FIG. 6. Changes in the Cu crystallite sizes occurring during reduction. The sizes were based on the width of the Cu(111) diffraction line data from the on-line, time resolved diffractograms in Fig. 4. Shown is also the FWHM of the line due to the overlapping CuO(111) and CuO(200) lines.

Whether there are still undetectable copper phases present in the reduced catalyst cannot be excluded, and a detailed understanding of this has to await the above mentioned quantitative XRD studies. However, it could be emphasized that XAFS studies on similar systems have failed to detect other Cu species than Cu metal (*22–26*). Thus, it can be concluded that if other Cu species are present they can only represent a small fraction of the total number of copper atoms.

After the reduction of CuO to Cu is complete, the Cu metal particles are not unexpectedly seen to continue to sinter (the line width decreases (Fig. 6) while the peak intensity increases, as seen in Fig. 4). It is, however, noteworthy that the rate of growth of the Cu particles appears to be significantly smaller in this region than in the reduction region. Consequently, other processes than sintering may contribute to the observed changes in the Cu particle size in the reduction region. For example, it is possible that the smallest CuO particles are preferentially reduced first. Furthermore, it is also possible that the nucleation process favors formation of smaller Cu particles at lower temperatures. In principle, a more detailed investigation of the CuO diffraction lines may give information on the former of these processes, but since all the intense CuO lines overlap with lines from ZnO or with other CuO lines (e.g., the CuO(111) and CuO(200) lines), it is for the present system difficult to give an exact value for the crystallite size for the CuO phase before or during reduction. Nevertheless, from an analysis of the total width of the peak due to the overlapping CuO(111) and CuO(200) lines, it is possible to get an idea of relative change in the CuO crystallite size. The width of this line (Fig. 6) does not seem to change significantly during reduction indicating that the size of the CuO crystallites apparently stays relatively constant. A more detailed analysis of this and other 2θ regions is desirable since it could also give information on

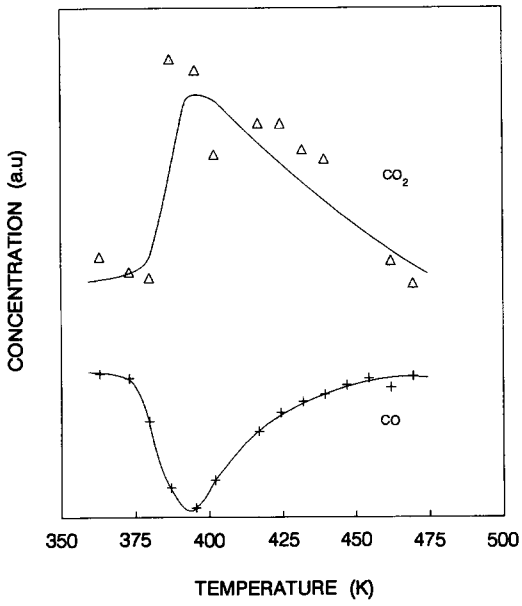

FIG. 7. Variation in the CO and CO_2 concentrations at the exit of the *in situ* cell during reduction of the catalyst with Cu/(Cu + Zn) = 0.80. The reduction gas consisted of 0.25% CO, 0.25% Co_2, 4% H_2, and balance Ar.

the changes occurring with the ZnO phase.

The Cu metal particle size of the binary catalyst at the final stage of the reduction is found to be about 14 nm (Fig. 6). This is significantly larger than that observed for the ternary catalyst with approximately the same Cu/Zn ratio. The smaller particle size in the ternary catalyst is presumably due to the alumina which is present as X-ray amorphous structures and probably acts as a highly dispersed well distributed textural promoter keeping the Cu particles apart and thereby minimizing sintering.

Figure 7 shows the variation in the CO and CO_2 concentrations at the exit of the reaction cell during reduction. The initial drop in the CO concentration and the parallel increase in the CO_2 concentration are presumably due to a consumption of CO to reduce the copper oxide forming Cu metal and CO_2. As soon as metallic Cu is formed the water gas shift reaction occurs utilizing the water formed in the reduction of the copper oxide with H_2. Above the temperature where the reduction is complete a continued slow increase in the CO concentration and a concurrent decrease in the CO_2 concentration are observed, indicating an apparent parallel decrease in the rate of the water gas shift reaction. This decrease may therefore be a result of the decrease in active area as a result of the observed sintering of the Cu metal particles. This conclusion is also supported by studies of single crystal surfaces and model systems (*38*), which indicate that the water gas shift activity is related to the Cu metal surface area.

5. CONCLUSION

The reaction cell described enables XRD studies of structural properties and *simultaneous* measurements of the catalytic reactivity of the *same* material. The design is simple, and the chemical inertness of the glass material makes it very attractive for most catalytic reactions. The unique advantages of the capillary tubes, including their plug flow geometry, result in a situation where direct relationships between catalytic activity and structural properties may be established. The use of a position sensitive detector makes the setup especially applicable for studies of dynamic transformations not only in heterogeneous catalysis, but also in other areas such as solid-state chemistry, electrochemistry, corrosion, and materials science. The extreme rapid temperature response of the reaction cell makes it well suited for studies of solid-state transformations. By use of the *in situ* XRD cell, we have been able to follow the phase transformations occurring in water gas shift and methanol catalysts during activation and at synthesis conditions. Specifically, the results show that in typical methanol catalysts the metallic copper phase, which is the only crystalline copper phase observed during synthesis conditions, is primarily formed from the CuO phase present in the calcined state. The size of the copper particles is found to increase during reduction, which explains the observed decrease in the rate of the water gas shift reaction.

ACKNOWLEDGMENTS

The authors are grateful to HASYLAB for offering beam time at the D4 beam line and to Dr. U. Löchner, Technische Hochschule Darmstadt, for helpful suggestions in connection with the heating of the glass capillaries. We are grateful to S. L. Jørgensen, B. S. Hammershøi, and S. L. Andersen for preparation of samples, provision of the test reactor data, and for many fruitful discussions. S. R. Møller is thanked for technical assistance. We also acknowledge financial support from the Danish Center for Surface Reactivity and from the Danish Academy of Technical Sciences (ATV).

REFERENCES

1. Owen, E. A. and Williams, E. St. J., *Proc. Phys. Soc. London* **56,** 52 (1944).
2. Long, R. W., US patent 2,483,500 (1947).
3. Gerward, L., Mørup, S., and Topsøe, H., *J. Appl. Phys.* **47,** 822 (1976).
4. Nandi, R. K., Pitchai, R., Wong, S. S., Cohen, J. B., Burwell, Jr., R. L., and Butt, J. B., *J. Catal.* **70,** 298 (1981).
5. Shiryaev, P. A., Kushnerev, M. Ya., Shashkin, D. P., and Krylov, O. V., *Kinet. Katal.* **23**(5), 1280 (1982).
6. Siryaev, P. A., Shashkin, D. P., Zurmukhtashvili, M. Sh., Margolis, L. Ya., and Krylov, O. V., *Kinet. Katal.* **25**(5), 1164 (1984).
7. Gavra, Z., and Murray, J. J., *Rev. Sci. Instrum.* **57** (8), 1590 (1986).
8. Jiang, X.-Z., Song, B.-H., Chen, Y., and Wang, Y.-W., *J. Catal.* **102,** 257 (1986); A similar cell was described by Topsøe, H., *in* "Experimental Methods for Solving Problems in Catalysis," Report to Ministry of Chemical Industry, Beijing, April 1980.
9. Kriger, T. A., Tarasova, D. V., Plyasova, L. M., Shkarin, A. V., and Stroeva, S. S., *React. Kinet. Catal. Lett.* **34,** 207 (1987).
10. Nix, R. M., Rayment, T., Lambert, R. M., Jennings, J. R., and Owen, G., *J. Catal.* **106,** 216 (1987).
11. Vong, M. S. W., Sermon, P. A., Self, V. A., Grant, K., and Blackburn, A. J., *J. Phys. E.* **21,** 495 (1988); Vong, M. S. W., Sermon, P. A., and Grant, K., *Catal. Lett.* **4,** 15 (1990).
12. Mamott, G. T., Barnes, P., Tarling, S. E., Jones, S. L., and Norman, C. J., *Powder Diffr.* **3,** 234 (1988).
13. Maddox, P. J., Stacharski, J., and Thomas, J. M., *Catal. Lett.* **1,** 191 (1988).
14. Ritter, J. J., *Powder Diffr.* **3,** 30 (1988).
15. Peiser, H. S., Rooksby, H. P., and Wilson, A. J. C., Eds., "X-ray Diffraction by Polycrystalline Materials," Chap. 3. The Institute of Physics, London, 1955.
16. Fabius, B., Feidenhans'l, R., Steffensen, G., Villadsen, J., and Clausen, B. S., Poster presented at "Nordisk Strukturkemiker Møde," University of Copenhagen, Jan. 1990.
17. Clausen, B. S., Steffensen, G., Møller, S. R., Fabius, B., Villadsen, J., Feidenhans'l, R., and Topsøe, H., *in* "HASYLAB Annual Report 1990," p. 593. HASYLAB, Hamburg, 1991.
18. Klier, K., *Appl. Surf. Sci.* **19,** 267 (1984).
19. Notari, B., *in* discussion section following Herman, R. G., Simmons, G. W., and Klier, K., "Proceedings, 7th International Congress on Catalysis, Tokyo 1980" (T. Seiyama and K. Tanabe, Eds.), p. 487. Kodansha, Ltd., Tokyo, 1980.
20. Chinchen, G. C., Waugh, K. C., and Whan, D. A., *Appl. Catal.* **25,** 101 (1986).
21. Burch, R., Golunski, S. E., and Spencer, M. S., *Catal. Lett.* **5,** 55 (1990).
22. Tohji, K., Udagawa, Y., Mizushima, T., and Ueno, A., *J. Phys. Chem.* **89,** 5671 (1985).
23. Clausen, B. S., Lengeler, B., Rasmussen, B. S., Niemann, W., and Topsøe, H., *J. Phys.* **C8,** 237 (1986).
24. Neils, T. L., and Burlitch, J. M., *J. Catal.* **118,** 79 (1989).
25. Clausen, B. S., Steffensen, G., Hyldtoft, J., Niemann, W., and Topsøe, H., *in* "X-ray absorption fine structure" (S. S. Hasnain, Ed.) p. 467. Ellis Horwood, Ltd., London, 1991.
26. Clausen, B. S., and Topsøe, H., *Catal. Today* **9,** 189 (1991).
27. Shimomura, K., Ogawa, K., Oba, M., and Kotera, Y., *J. Catal.* **52,** 191 (1978).
28. Duprez, D., Ferhat-Hamida, Z., and Bettahar, M. M., *J. Catal.* **124,** 1 (1990).
29. Chinchen, G. C. and Waugh, K. C., *J. Catal.* **97,** 280 (1986).
30. Bowker, M., Hadden, R. A., Houghton, H., Hyland, J. N. K., and Waugh, K. C., *J. Catal.* **109,** 263 (1988).
31. Rostrup-Nielsen, J. R. and Højlund Nielsen, P. E., *in* "Deactivation and Poisoning of Catalysts" (J. Oudar and H. Wise, Eds.) p. 259. Marcel Dekker, Inc., New York, 1985.
32. Frost, J. C., *Nature (London)* **334,** 577 (1988).
33. Nonneman, L. E. Y., and Ponec, V., *Catal. Lett.* **7,** 213 (1990).
34. Burch, R., Golunski, S. E., and Spencer, M. S., *J. Chem. Soc. Faraday Trans.* **86**(15), 2683 (1990).
35. Clausen, B. S., Lengeler, B., and Rasmussen, B. S., *J. Phys. Chem.* **89,** 5671 (1985).
36. Nielsen, A., "An Investigation of Promoted Iron Catalysts for the Synthesis of Ammonia." J. Gjellerup, Copenhagen, 1950.
37. Clausen, B. S., Mørup, S., Topsøe, H., Candia, R., Jensen, E. J., Baranski, A., and Pattek, A., *J. Phys.* **C6,** 245 (1976).
38. Champbell, C. T. and Daube, K. A., *J. Catal.* **104,** 109 (1987).